

This article was downloaded by:

On: 22 January 2011

Access details: *Access Details: Free Access*

Publisher *Taylor & Francis*

Informa Ltd Registered in England and Wales Registered Number: 1072954 Registered office: Mortimer House, 37-41 Mortimer Street, London W1T 3JH, UK



## The Journal of Adhesion

Publication details, including instructions for authors and subscription information:

<http://www.informaworld.com/smpp/title~content=t713453635>

### Graphite Fiber Treatments which Affect Fiber Surface Morphology and Epoxy Bonding Characteristics

R. J. Dauksys<sup>a</sup>

<sup>a</sup> Air Force Materials Laboratory Composites and Fibrous Materials Branch, Wright-Patterson Air Force Base, Ohio, U.S.A.

**To cite this Article** Dauksys, R. J.(1973) 'Graphite Fiber Treatments which Affect Fiber Surface Morphology and Epoxy Bonding Characteristics', *The Journal of Adhesion*, 5: 3, 211 – 244

**To link to this Article:** DOI: 10.1080/00218467308075021

**URL:** <http://dx.doi.org/10.1080/00218467308075021>

PLEASE SCROLL DOWN FOR ARTICLE

Full terms and conditions of use: <http://www.informaworld.com/terms-and-conditions-of-access.pdf>

This article may be used for research, teaching and private study purposes. Any substantial or systematic reproduction, re-distribution, re-selling, loan or sub-licensing, systematic supply or distribution in any form to anyone is expressly forbidden.

The publisher does not give any warranty express or implied or make any representation that the contents will be complete or accurate or up to date. The accuracy of any instructions, formulae and drug doses should be independently verified with primary sources. The publisher shall not be liable for any loss, actions, claims, proceedings, demand or costs or damages whatsoever or howsoever caused arising directly or indirectly in connection with or arising out of the use of this material.

# Graphite Fiber Treatments which Affect Fiber Surface Morphology and Epoxy Bonding Characteristics†

R. J. DAUKSYS

*Air Force Materials Laboratory Composites and Fibrous Materials Branch  
Wright-Patterson Air Force Base Ohio 45433, U.S.A.*

*(Received November 22, 1972)*

Means of inducing carbonyl functional groups to high modulus graphite fibers (Thornel 50) are described. One approach involves wet chemical oxidation of the fibers in aqueous sodium iodate solution. Another route to hypothesized augmented carbonyl functionality on graphite fibers proceeds through reaction of the fibers in an aqueous dioxane osmium tetroxide solution. In the latter case, coupling of graphite carbonyl to oxirane epoxy is postulated as occurring through an intermediate stannic chloride complex. Bonding of fibers to matrix is shown to be improved with little to no loss in tensile properties of the fibers.

As a result of the specificity of the reactions, the surface characteristics of the graphite fibers are revealed when viewed with high magnification scanning electron microscopy (SEM). Based on such observations, a model of the fiber is diagrammed as a compromise of a fibrillar structure and ordered crystallites with tilt and sub-grain boundaries.

Also described is a thermal oxidative, polymeric coating treatment which showed modest success in improving graphite fiber/epoxy matrix bonding. Fractured composites in this phase of study indicated unusual fiber anomalies in the form of rod-like extensions from the internal portion of individual graphite filaments.

## I INTRODUCTION

Higher elastic modulus graphite fibers show an increasingly higher degree of fiber anisotropy and this has a marked influence on reducing transverse

† Presented at the Symposium on "Interfacial Bonding and Fracture in Polymeric, Metallic and Ceramic Composites" at the University of California at Los Angeles, Nov. 13-15, 1972. This Symposium was jointly sponsored by the Polymer Group of S. California Section, ACS and Materials Science Department, U.C.L.A.

composite properties. Also, the interlaminar shear in epoxy composites tends to be lower. Composite shear strength† is important to the attainment of good composite strength properties, and it also affects the mode of composite failure. In some cases, an excellent bond (one which provides a high shear strength value) can be detrimental to certain composite properties if a brittle type of failure results. Thus, high composite shear strengths should generally be accompanied by toughness.

There are many theories and hypotheses concerning improvement of the fiber-matrix bond. Chemical coupling, complete wetting of fiber surface, low matrix contact angle, fiber porosity, high fiber surface area, etc., probably all contribute to good bonding (good interlaminar shear strength) where the type and extent to which these factors operate are dependent on the characteristics of fiber and matrix.

In this paper, three graphite fiber treatments are discussed which result in higher values of composite interlaminar shear strengths compared to initial polyvinyl alcohol (PVA) or H<sub>2</sub>O sized fibers. One method involves a thermal-oxidative treatment of the fibers used in conjunction with a polymeric coating, prior to epoxy impregnation. The other two are low temperature, wet chemical oxidations that induce carbonyl specificity to the graphite surface which react, through an intermediate complex, to epoxy molecules.

## II COMPOSITE CONSTITUENTS

### 1 Epoxy‡

An intermediate modulus ( $500 \times 10^3$  psi) epoxy resin was used as a control matrix (Table I). The resin, designated ERL 2256, is composed of a mixture of a diglycidylether of bisphenol A diluted with 37.5% bis 2, 3-epoxy-cyclopentyl ether. The hardener, ZZL 0820, is m-phenylene diamine and dimethylaniline mixture.

### 2 Reinforcement§

The graphite yarn used was Thornel 50 (modulus of elasticity  $50 \times 10^6$  psi) with polyvinyl alcohol or water sizing. The yarn was bi-plyed, 720 filaments

† Shear strength is taken as a measure of the interfacial efficiency between matrix and reinforcement. Caution must be used in interpreting results of this kind as a high value does not necessarily indicate an optimum system.

‡ Union Carbide Corporation.

§ Sears, Roebuck and Company.

per ply. Also, a small amount of a high modulus, experimental yarn, designated Thornel 80 ( $80 \times 10^6$  psi modulus, PVA size) was heat treated-polymer coated.

### III HEAT TREATMENT-POLYMERIC COATING PROCESS

#### 1 Heat treatment

High temperature oxidation of graphite fibers has been shown to augment the chemical functionality of the surface, thereby presumably imparting reactive sites to chemically couple with reactive groups on various polymeric matrices. It is known that lower modulus yarns of the same precursor filaments and generally same external physical fiber morphology, induce higher composite shear strength values. For example, low modulus Thornel 25 ( $25 \times 10^6$  psi modulus) results in a higher composite shear strength than Thornel 50 ( $50 \times 10^6$  psi modulus) by a factor of 1.5. For a carbon yarn ( $12 \times 10^6$  psi modulus)/epoxy composite the increase is substantial at a factor of three or greater.

Two methods were used to heat treat the graphite yarn prior to application of the thermoplastic polymeric coating and epoxy impregnation. In one instance a propane flame generated from a Craftsman† 14.1-ounce propane fuel tank was used. A schematic of the process is shown in Figure 1. Temperature was not monitored, but the yarn was pulled through the hot part of the flame which is known to be  $1925^\circ\text{C}$ .

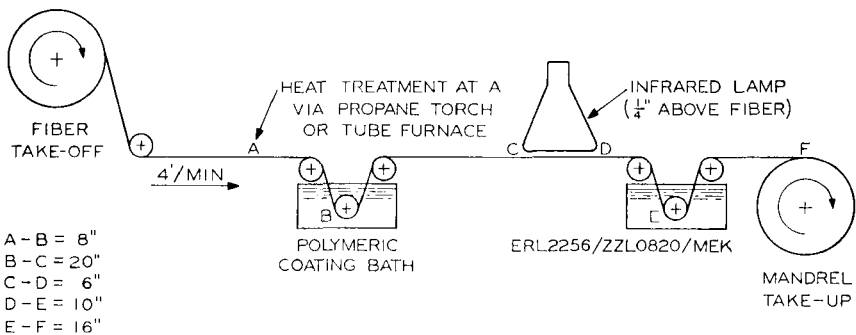


FIGURE 1 Heat treatment-polymeric coating.

In the second case, a tube furnace 1 foot long, and  $\frac{1}{2}$ -inch in diameter was positioned in place of the propane tank. Thermoplastic coatings, epoxy impregnation, and speed of yarn pull-through were as depicted in Figure 1. The maximum temperature obtainable (1000°F) was used in all of the heat treatments involving the tube furnace. As no beneficial effects resulted, this ramification of the process is not discussed further.

It was surmised that in addition to the fiber oxidation which takes place during the heat treatment, the temperature and gaseous pressure generated may serve to decompose foreign contaminants and dispel them from the fiber surface; thus, more intimate contact between fiber and matrix.

A third effect would be increased porosity, due to sublimation or volatilization of absorbed low molecular weight material within the pores of the fiber. Didchenko<sup>1</sup> shows for Thornel 40 (fiber modulus of  $40 \times 10^6$  psi) that a chromic acid treatment did not necessarily increase total pore volume, but did increase the frequency of the large size pores. In both instances; adhesive bonding may be increased by a mechanical "hooking" effect.<sup>2</sup>

An adverse consequence would be fiber degradation leading to lower composite strength properties.

TABLE I

Properties of ERL 2256/ZLL 0820 matrix and polymeric coatings

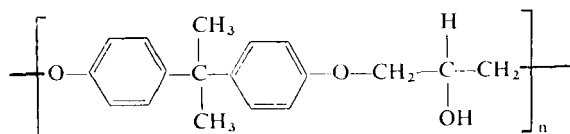
Cast properties of ERL 2256/ZLL 0820 epoxy resin <sup>a</sup>	
Tensile strength	$14.5 \times 10^3$ psi
% elongation at proportional limit	1-2%
% elongation at failure	6.5%
Flexural strength	$22.5 \times 10^3$ psi
Flexural modulus	$527 \times 10^3$ psi
Specific gravity	1.22
Heat distortion	145-150°C
Properties of a moulded polyhydroxy ether <sup>a</sup>	
Tensile strength	$9.5 \times 10^3$ psi
% elongation at yield	3-5%
Flexural strength	$14.5 \times 10^3$ psi
Flexural modulus	$4.1 \times 10^5$ psi
Specific gravity	1.182
Heat distortion	188°F
Cast properties of polyphenylene oxide (P <sub>3</sub> O) <sup>b</sup>	
Tensile strength	$6-10 \times 10^3$ psi
% elongation at yield	2-5%
Tensile modulus	$350-450 \times 10^3$ psi
Specific gravity	1.14-1.117
Glass transition ( $T_g$ )	230°C

<sup>a</sup> Ref. Bakelite Product Data Bulletins, Union Carbide Corp.

<sup>b</sup> P<sub>3</sub>O Film Properties, General Electric Company, 15 Jan. 1969

## 2 Polymeric coatings

a. *Polyhydroxy ether*† (PHE) A polyhydroxy ether (PHE) of the form was used for initial treatment evaluations. The PHE was applied in various



solutions differing in amount of PHE, as well as type of solvent. Molded properties of PHE are shown in Table I. Formulations of interest are shown in Table II.

TABLE II  
Polymeric coating solutions

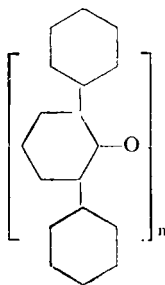
Solution number	% by weight polymer	Solution
1	0.91	1 gram polyhydroxy ether (PHE) 118 ml. cellosolve
2	0.80	1 gram (PHE) 128 ml. cellosolve acetate
3	1.72	2 grams (PHE) 125 ml. cellosolve
4	1.66	2 grams (PHE) 125 ml. cellosolve acetate
5	3.45	4 grams (PHE) 125 ml. cellosolve
6	3.3	4 grams (PHE) 125 ml. cellosolve acetate
7	11.4	10 grams polyphenylene oxide (P <sub>3</sub> O) 100 ml. benzene
8	1.4	1 gram P <sub>3</sub> O 100 ml. benzene
9	2.3	2 grams P <sub>3</sub> O 100 ml. benzene
10	3.4	3 grams P <sub>3</sub> O 100 ml. benzene

b. *Polyphenylene oxide*‡ (P<sub>3</sub>O) The second coating resin was an experimental thermoplastic (shown below) designated poly 2, 6 diphenyl-1,

† Union Carbide Corporation.

‡ General Electric.

4-phenylene oxide.<sup>3</sup> Table I shows some of the properties characteristic of the resin, and Table II shows the various formulations in benzene as the solvent. Note: The coatings were always applied after heat treatment or take-off and before the infrared lamp (solvent evaporation). See Figure 1.



The polymeric coatings were selected because it was surmised that the use of high molecular weight, long chain, thermoplastic materials of considerably greater elongation than the space network polymer, if applied in appropriate amounts, would not lessen composite properties, but would form a microductile area in the immediate vicinity of the interface. This transition zone (generally of lower modulus and higher elongation) could satisfactorily function as a:

1) stress relief medium which reduces compressive stresses caused by matrix shrinkage during cure, that on a macro level, especially at high volume fraction fiber could revert to tensile forces which form and propagate cracks.

2) crack inhibitor and/or arrestor by virtue of excess energy needed (compared to the highly cross-linked epoxy) for the crack to plastically deform, orient, and fracture long chain molecules. Simplistically, this means that Griffith's criterion for brittle fracture does not hold in this region and a plastic energy term needs to be added to his derivation due to reduction of stress concentrations at the tip of the crack (crack blunting). For a general reference of such phenomena, see Andrews.<sup>4</sup>

3) means of increasing the effective transfer length of fractured fibers thereby increasing the possibility of maximum transfer of imposed stress to the continuous fibers.

In the case of the polyhydroxy ether, the presence of pendent hydroxyl groups suggests a possible coupling reaction with the oxirane ring of the epoxy in the formation of an ether linkage, as well as reaction with carboxyl on the graphite fiber in the formation of an ester linkage, ergo, possible increased interlaminar shear strength.

### 3 Mechanical and physical property evaluations

a. *Short Beam Shear Test* Primarily due to its simplicity, the short beam shear test was used in this study as a means of determining whether a treatment enhances fiber/matrix bonding. The short beam test, especially if bonding is poor, will promote complex failures with specimens exhibiting combinations of tension, flexure, and shear. As coupling improves, the failure mode progresses from the complex type, to one of compression-tension, to one of tension which is usually quite brittle in nature. It should be mentioned that these observations have been made for Thornel series composites only.

The short beam samples (Figure 2) were cut (parallel to fiber orientation) from unidirectional panels,  $2\frac{1}{4}'' \times 2\frac{1}{4}''$  using a diamond wheel saw. Finished test specimens measured approximately  $1'' \times \frac{1}{4}'' \times 0.060''-0.070''$ . Specimens were tested at constant span-to-depth (S/D) ratios of 6/1 and 4/1, respectively. Crosshead speed was constant at 0.05 inches/minute. Shear strength was calculated from

$$\sigma = \frac{3P}{4Wt}$$

where  $\sigma$  = short beam shear strength (pounds/inches<sup>2</sup>)

P = load (pounds)

W = width (inches)

t = thickness (inches)

Tests were conducted at both 6/1 and 4/1 span-to-depth ratios. A minimum of four tests was conducted at both S/D's for each average value shown in the tables.

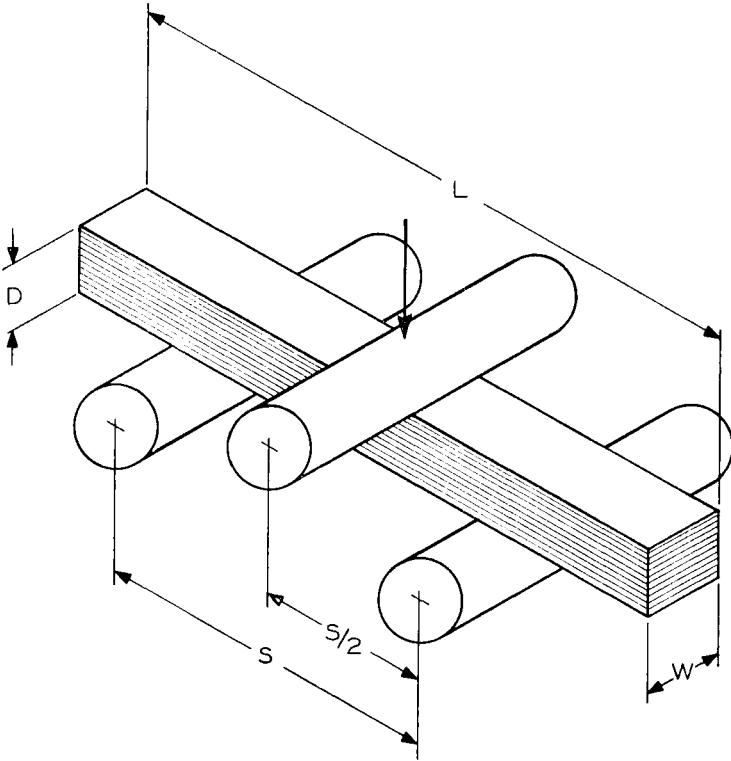
b. *Flexural Test* As in the case of shear, 3-point flexural specimens (Figure 2) were prepared from flat panel laminates. Unidirectional specimens were obtained from the square panels in essentially the same fashion as the short beam shear specimens. Overall panel dimensions were approximately  $2\frac{1}{4}'' \times 2\frac{1}{4}'' \times 0.060''-0.070''$ . A S/D ratio of 20/1 was used for all tests.

Composite flexural strength was determined from

$$\sigma = \frac{3SP}{2WD^2}$$



where  $\sigma$  = flexural strength (pounds/inches<sup>2</sup>)  
 $S$  = span (inches)  
 $P$  = load (pounds)  
 $W$  = width (inches)  
 $D$  = depth (inches)



## FLEXURAL TEST

$$L = 2\frac{1}{4}''$$

$$W = \frac{1}{4}''$$

$$S/D \approx 20/1$$

$$D = 10 \text{ PLIES, } 0.060'' - 0.070''$$

## SHORT BEAM SHEAR TEST

$$L = 1''$$

$$W = \frac{1}{4}''$$

$$S/D = 6/1 \text{ AND } 4/1$$

$$D = 10 \text{ PLIES, } 0.060'' - 0.070''$$

FIGURE 2 Flexural and short beam shear specifications.

modulus was calculated from

$$E = \frac{PS^3}{4WD^3}$$

where the symbols are as defined for the preceding flexural strength equation. Specimens were tested at a crosshead rate of 0.05 inches/minute. A minimum of three tests was conducted for each average value shown in the accompanying tables.

NOTE: Due to the limited amount of graphite fiber treated in the wet chemical oxidations, molded composites measured  $6'' \times \frac{1}{4}'' \times 0.60''-0.70''$  from which flexural and/or shear specimens were obtained.

c. *Volume % Fiber and Composite Density* The percentage of graphite fibers in cured composites was determined by a nitric acid dissolution method devised by Kuhbander.<sup>5</sup> Composites were subjected to concentrated nitric for approximately two hours at 140°F, or until after periodic changing of the acid, the solution remained clear indicating that the resin had dissolved. The remaining graphite fibers were then rinsed in water, dried, weighed, and volume fraction calculated, using measured fiber and cured matrix densities. Obvious limitations of this method are that a voidless composite must be assumed, and that densities of reinforcements and matrix must be reliable. Where a polymeric coating was applied, the quantity was considered negligible and therefore not entered as part of the calculations.

An average density of 1.62 g/cc was selected for the graphite, however the reader is cautioned that fiber density is nonuniform in lengths used in these composites and that the heat treatments described in this report probably reduce the fiber density.

Composite density was determined by water immersion.

#### 4 Composite fabrication

The following discussion describes the process steps used to treat and impregnate the graphite fibers. In subsequent sections detailed particulars shall be presented to complement the discussion.

Treatment of the continuous yarn was accomplished via the apparatus shown in Figure I. Generally, the yarn was pulled from a take-off mechanism, over a propane torch (with standard wingtip) generated flame, through a coating solution which consisted of a 0.8–11.5% by weight solution of organic

polymeric material in appropriate solvent, through approximately a 60% by weight solids solution of control matrix in methyl ethyl ketone, and finally over a mandrel covered with a Teflon coated glass fabric (Fluoroglas) where a monolayer tape was wound. The Teflon fabric served to act as a substrate for the prepreg tape, as well as to protect the mandrel. In most instances, two prepreg tapes were wound and thus two composite panels were fabricated utilizing the same fiber treatment parameters.

It should be mentioned that the propane flame heated the filaments to a dull red incandescence so that they could clearly be seen vibrating over the heat source. The pressure of the gas was enough to lift broken fibers.

Resin B-Stage normally took from 16–24 hours at room temperature after which the prepreg was removed from the mandrel. Subsequently, the tape was cut into  $2\frac{1}{4}'' \times 2\frac{1}{4}''$  plies and were layed up, ten deep, in a compression mold. After following the cure cycle shown below, the composite was removed and subjected to short beam shear and flexural tests.

- a) 2 hours at 180°F followed by (100 psi)
- b. 4 hours at 300°F at (100 psi)
- c) Slow cooling to R.T. (100 psi)

## 5 Composite properties

Table III presents data comparing “control” composites (composites fabricated with yarn that was not heat treated or polymer coated) to composites fabricated with yarn that was heat treated or polymer coated. For all practical purposes the composites fabricated with the heat treated or polymer coated yarn show no significant changes from the control composites.

Table IV indicates that improvements in composite interlaminar shear strength are possible if the propane flame heat treatment is used in conjunction with the various polymeric coating solutions outlined in Table II. For the most part, flexural properties of the composites do not appear to be deleteriously affected. Of particular note is the significant increase in shear strength for the laminate fabricated with the heat treated-polymeric coated Thornel 80 yarn compared to the Thornel 80 control composite ( $6.3 \times 10^3$  psi to  $2.5 \times 10^3$  psi, respectively).

## 6 Scanning electron microscopy evaluation

Figures 3 and 4 are of the “as-received”  $H_2O$  sized yarn at  $6000 \times$  and  $20,000 \times$ , respectively. Notice the smoothness of the surface even at the higher

TABLE III  
Flexural and shear properties of unidirectional Thornel/ERL 2256 composites  
control or heat treated only or polymer coated only yarn

Comp. no.	Remarks	Size	V/F %	Density g/cc	Flex E 10 <sup>6</sup> psi	Flex $\sigma$ 10 <sup>3</sup> psi	Short beam shear 6/1 10 <sup>3</sup> psi	Short beam shear 4/1 10 <sup>3</sup> psi
1	Thornel 50 control	PVA	66.1	1.52	19.8	110.7	3.4	3.8
2	Thornel 50 control	PVA	64.7	1.50	20.6	110.2	3.5	3.8
3	Thornel 50, propane flame only	PVA	67.1	1.52	18.1	109.1	3.7	4.0
4	Thornel 50, propane flame only	PVA	65.9	1.52	19.7	114.4	3.8	4.0
5	Thornel 50 control	H <sub>2</sub> O	64.1	1.47	18.8	110.4	3.4	3.6
6	Thornel 80 <sup>a</sup> control	PVA	60.0	1.67	28.0	125.0	—	2.5
7 <sup>b</sup>	No heat treat, polymer coated only	H <sub>2</sub> O or PVA	63.1	1.47	20.2	116.5	3.5	3.7

<sup>a</sup> Thornel 80—Modulus of  $80 \times 10^6$  psi

<sup>b</sup> Results of *all* composites fabricated with polymer coated yarn, but not heat treated.

TABLE IV  
Flexural and shear properties of unidirectional Thornel/ERL 2256  
composites heat treated—polymer coated yarn

Comp. no.	Remarks	V/F %	Density g/cc	Flex E 10 <sup>6</sup> psi	Flex O 10 <sup>3</sup> psi	Short beam shear 6/1 10 <sup>3</sup> psi	Short beam shear 4/1 10 <sup>3</sup> psi
8	A, Solution 1	64.5	1.48	19.3	127.1	5.4	7.1
9	A, Solution 2	64.4	1.52	19.5	110.6	5.4	6.9
10	A, Solution 3	59.6	1.48	17.7	71.3	5.4	6.8
11	A, Solution 4 <sup>a</sup>	57.4	1.44	19.1	71.5	4.9	6.8
12	A, Solution 5	64.3	1.46	19.2	104.7	4.7	6.2
13	A, Solution 6	62.2	1.48	19.0	101.6	5.1	6.4
14	A, Solution 7	61.7	1.46	19.6	99.3	6.2	6.8
15	B, Solution 8	60.9	1.46	16.9	71.6	5.3	6.6
16	A, Solution 9	62.0	1.46	20.0	111.2	7.2	7.5
17	A, Solution 10	62.5	1.45	17.8	81.7	5.2	6.3
18	B, Solution 1	65.2	1.50	19.6	100.1	4.4	5.0
19	B, Solution 9	57.0	1.44	18.5	90.7	5.9	7.7
20	C, 2% PHE in cellosolve acetate + MEK	59.3	1.62	28.7	121.0	—	6.3

<sup>a</sup> A = Thornel 50 (PVA size), B = Thornel 50 (H<sub>2</sub>O size), C = Thornel 80 (PVA size). Propane flame 2.5" below yarn.

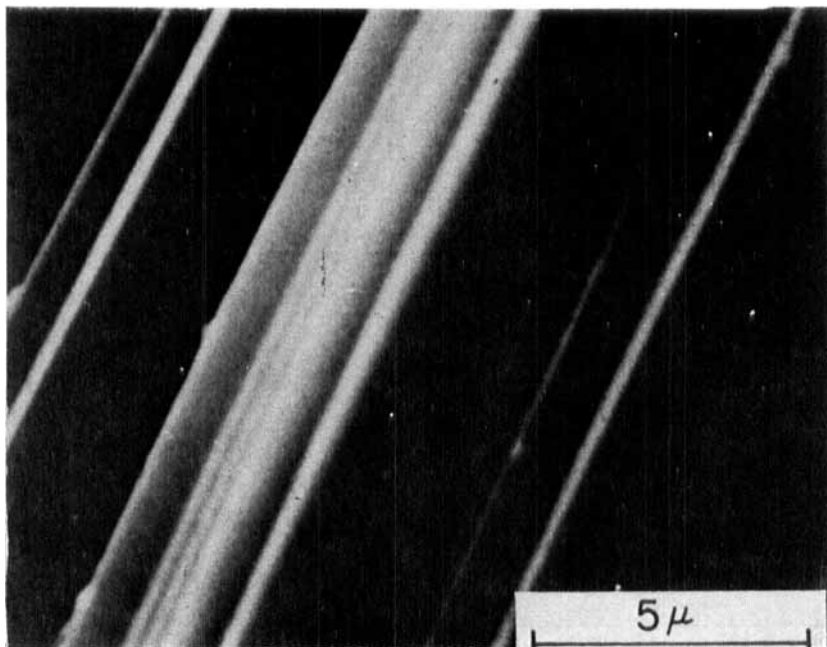


FIGURE 3 As-received Thornel 50, H<sub>2</sub>O-sized yarn.

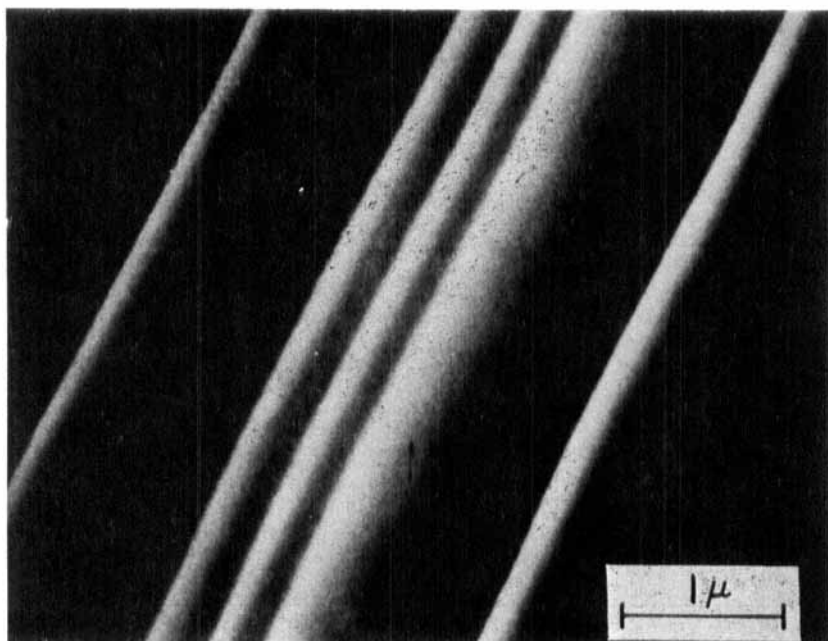


FIGURE 4 As-received Thornel 50, H<sub>2</sub>O-sized yarn.

magnification. SEM micrographs of PVA sized fibers appear no different.

Figure 5 shows a fiber from H<sub>2</sub>O sized yarn that was passed through the blue tip of a propane torch generated flame (1925°C) at a rate of 4 feet per minute. The oxidation process at this temperature and rate is enough to cause "pip" markings on the surface, as well as in some instances actual expulsion of the material. The general population of the bundle consisted of more fibers with raised material (pips) indicating expansion of gases within pores.

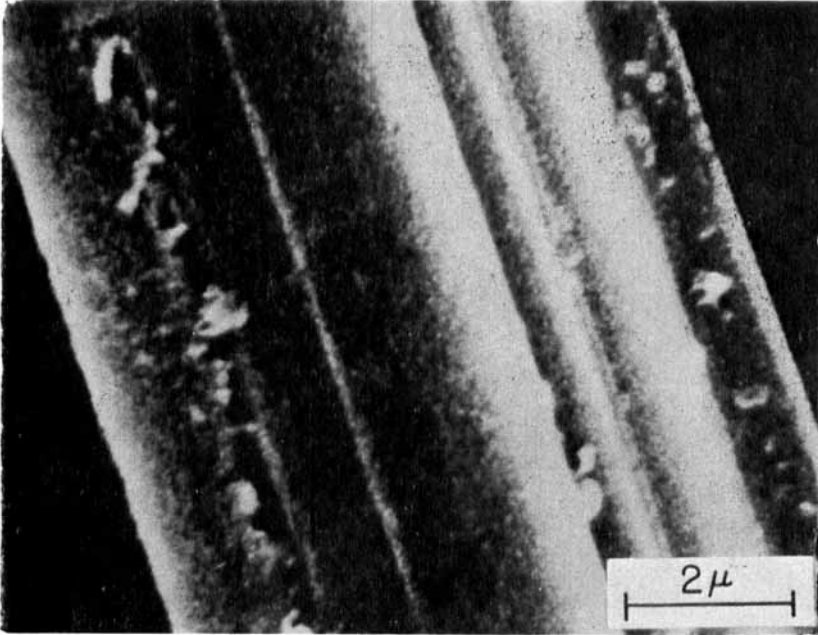


FIGURE 5 Thornel 50; heat treated (propane flame) at 4 feet/min.

Figure 6 depicts three fibers from a yarn that was heat treated by sweeping a propane flame back and forth over a four-inch length for 10 seconds. The fibers were more smooth than the four feet/minute treatment; however, large elliptical depressions ranging from approximately 0.8 to 2.5 microns along the major axis were observed.

Composite 20, tested by short beam shear, is represented in Figures 7 and 8. The lower magnification shows the gradual transition from the compression face (left side of figure) to the tension side of the composite. At higher magnification we may observe fiber bundle debonding rather than individual fiber pull out.

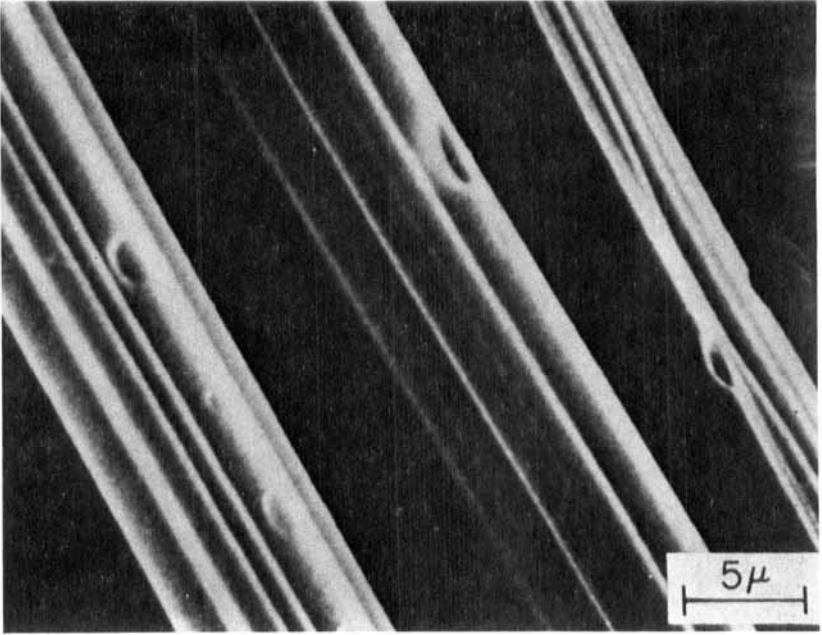


FIGURE 6 Thornal 50; heat treated (propane flame) for 10 sec.

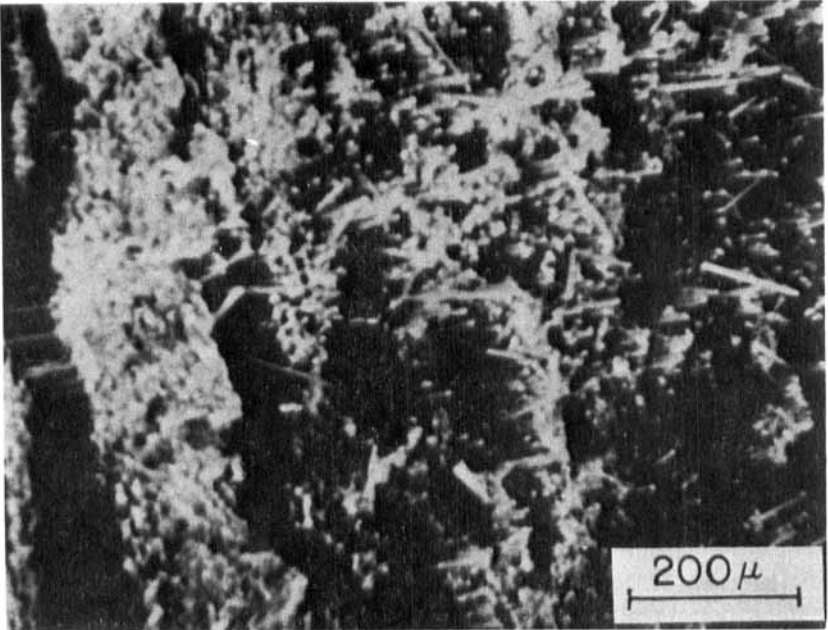


FIGURE 7 Composite 20;  $80 \times 10^6$  psi filament.

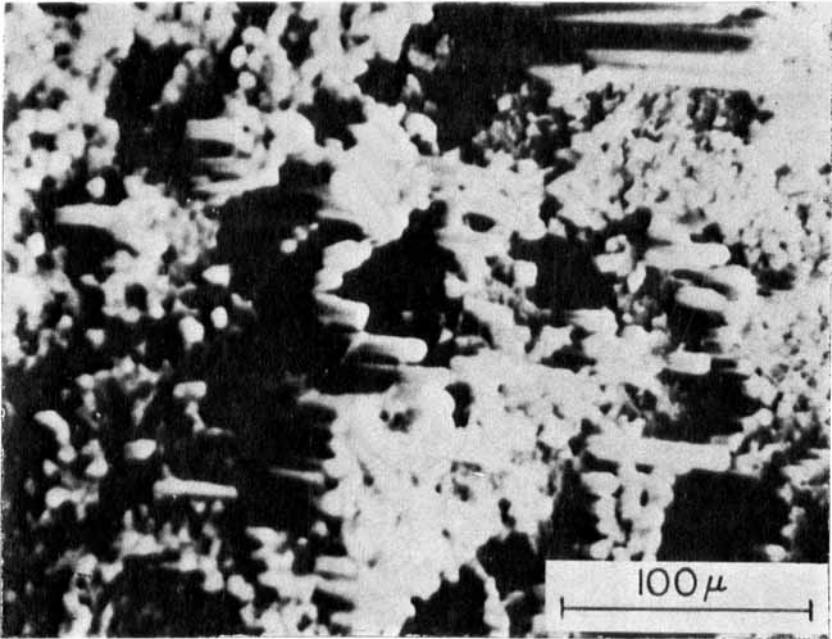


FIGURE 8 Composite 20;  $80 \times 10^6$  psi filament.

Low composite shear strength is usually accompanied by complex failures where at ultimate load the specimen assumes a deformed shape, but does not fracture through. Control composites failed in like manner.

Figure 9 shows the fracture surface of Composite 16 which was of both good flexure strength ( $110 \times 10^3$  psi) and shear strength ( $7.5 \times 10^3$  psi).

Figures 10 and 11 show close up views of fractured surfaces of Composites 16 and 20, respectively, where rope-like fibrils seem to be pulled from the interface area. Although no count was taken, this effect was observed over a great deal of the fractured composite area in both compression and tension zones. At first the writer thought the fibrils were the result of some phenomenon associated with the polymeric coating, as the majority of them appeared to originate at interfacial zones; however, on scanning Composite 20 filament modulus =  $80 \times 10^6$  psi), the area shown in Figure 12 dispelled that consideration.

Figure 12 shows conclusively that the origin of the fibril is from the graphite fiber itself—an indication that the graphitization processes that produced the  $H_2O$  sized  $50 \times 10^6$  psi modulus filament, as well as the  $80 \times 10^6$  psi modulus fiber, were nonuniform.



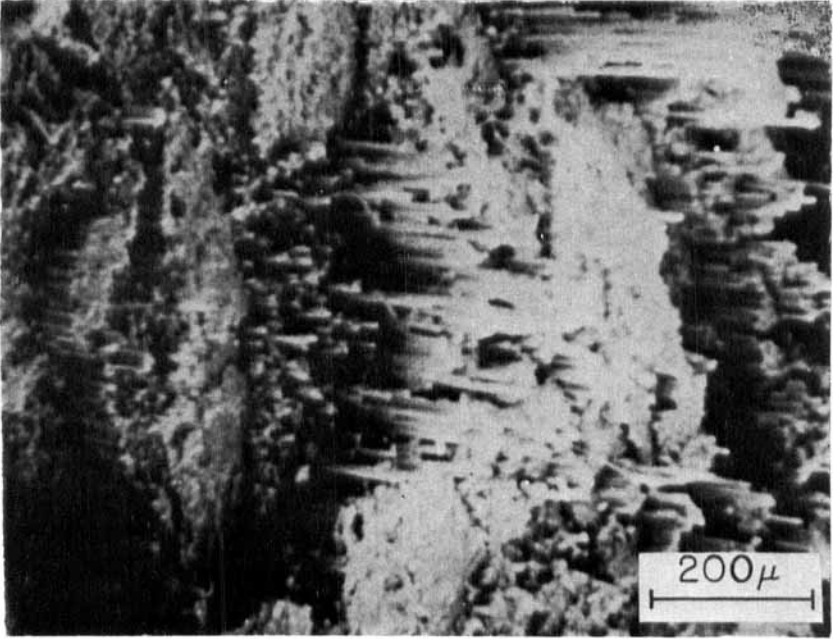


FIGURE 9 Composite 16.

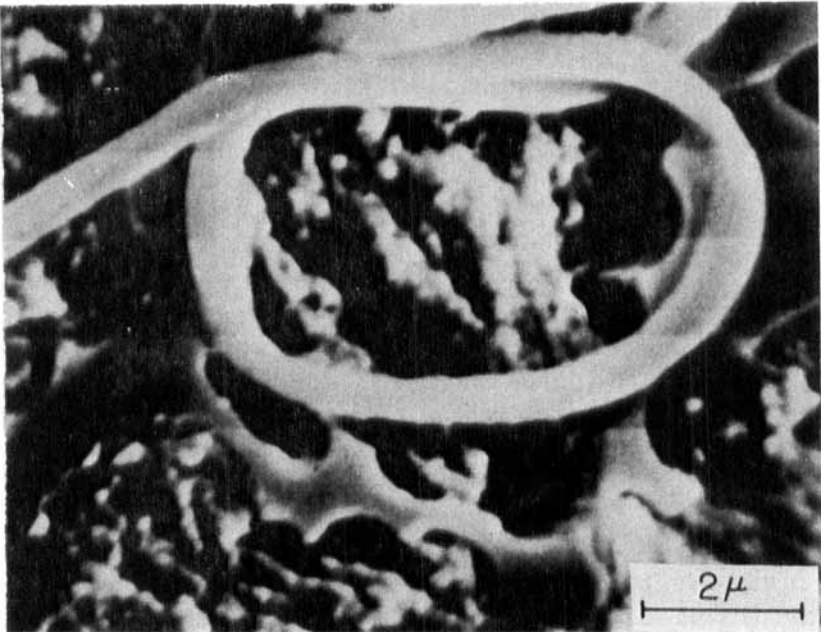


FIGURE 10 Composite 16; note fibril.

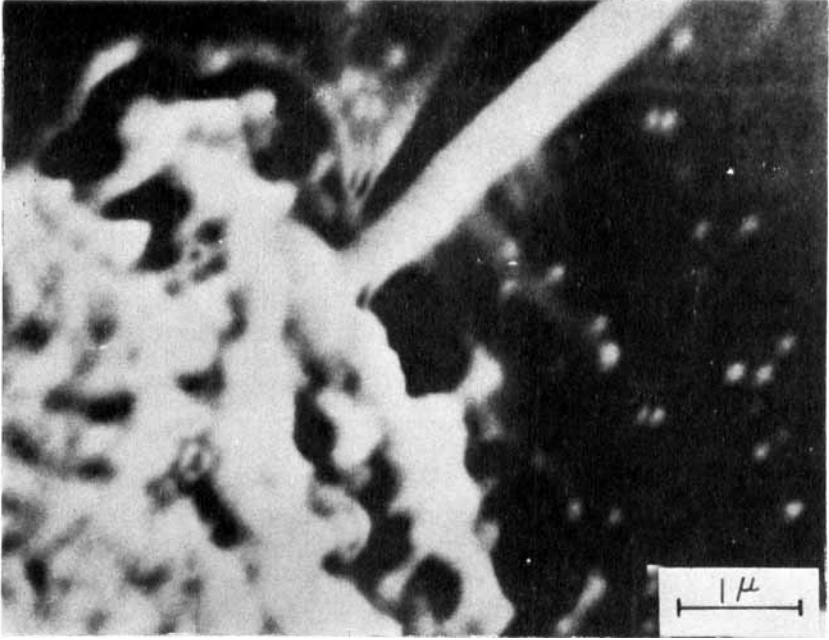


FIGURE 11 Composite 20; fibril appears to be at interface.

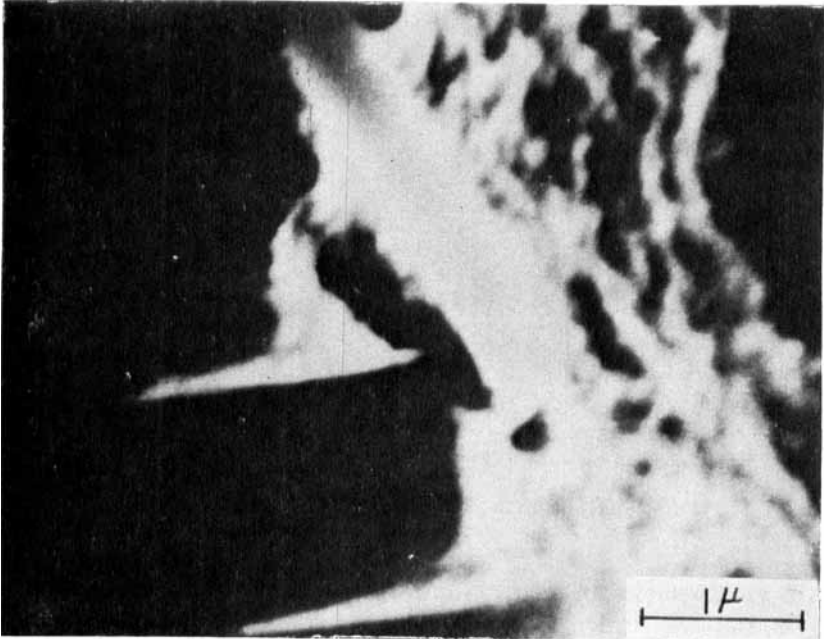


FIGURE 12 Composite 20; fibril emanating from fiber.

The fibrils may be composed of compositions varying from the starting precursor material to some intermediate form of the Thornel 50. Whatever the case, it is evident that the fibrils are of higher elongation and are not bonded to the surrounding "graphitic" material.

Extension of the fibrils may take place as the composite is loaded. The fibrils are strained and molecular flow results to relieve the imposed stress. At the ultimate strength of the composite, the ultimate strain in the fibril is still not achieved. At an infinitely small period of time after composite failure, the maximum strain in the fibril (elongation is maximum) is achieved, and it fractures. Johnson<sup>6</sup> shows a SEM photomicrograph of a polyacrylonitrile precursor fiber which looks remarkably like the onset of the aforementioned flawed graphitized precursors.

Figure 13 is the last of the series showing a fibril of approximately  $40\ \mu$  (0.0017 inches) in length.

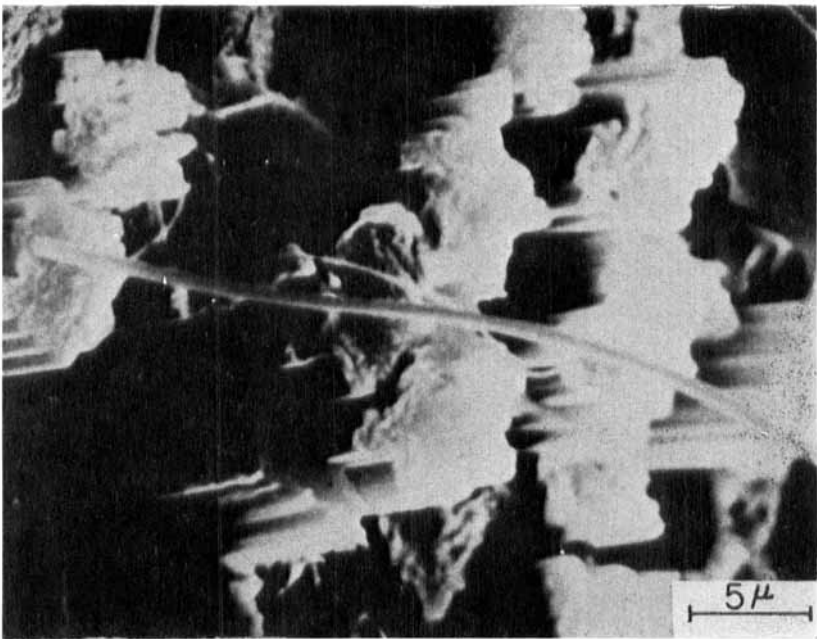


FIGURE 13 Composite 20; note length of fibril.

Figure 14 shows an internal void with sharp ridges resembling cracked areas, this observation was only noted for a very few fibers in the same general area.

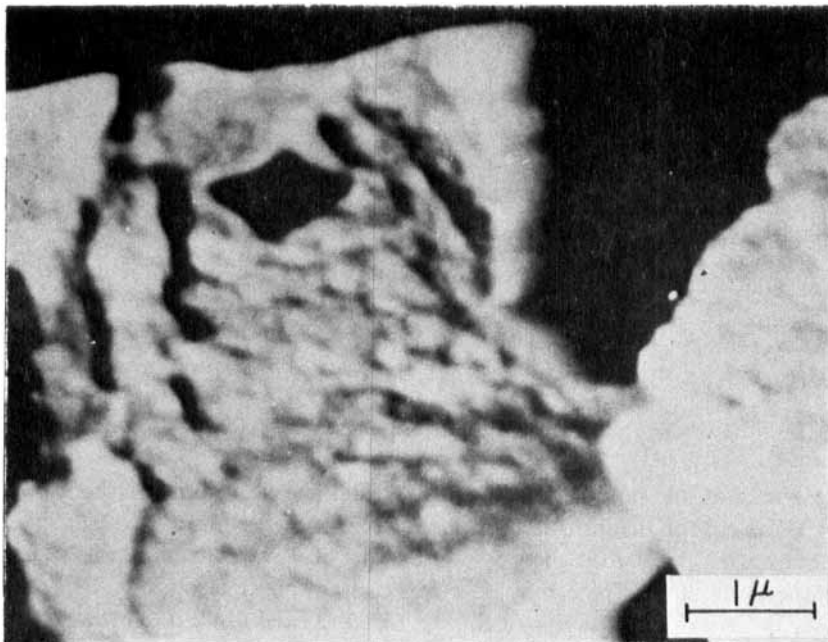


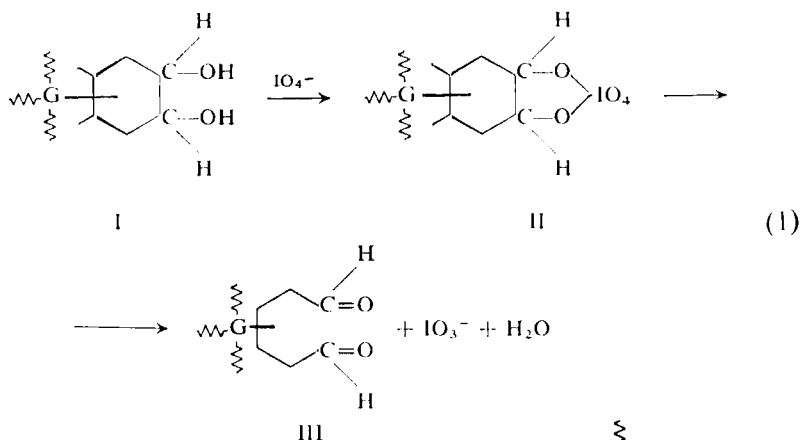
FIGURE 14 Composite 16; note diamond shaped hole and longitudinal depressions.

## IV CHEMICAL PROCEDURES

### 1 Malaprade reaction

Malaprade<sup>7</sup> as a result of his study, concluded that reactions involving 1, 2-diols with certain oxidizers were most specific in the formation of carbonyls. Monofunctional aldehydes, alcohols, and ketones are inert or react slowly. Wiberg<sup>8</sup> mentions that oxidation of some aromatic phenols is also possible. The mechanism of cleavage of the 1, 2-diol proceeds through a diol-oxidant complex where the oxidant must contain a central atom with two electrons in the outer shell that may bridge to the oxygen atoms of the hydroxyls. The iodate ion is a choice candidate. Complexing eventually results in carbonyl formation with reduction of iodate to iodite.

In view of Malaprade's study of the conversion of 1,2-diols to carbonyls, and in light of previous hypotheses regarding the chemical functionality of the graphite fiber surface, the writer postulates that the surface contains groups of 1,2-diols that are susceptible to cleavage when subjected to an aqueous solution of sodium iodate ( $\text{NaIO}_4$ ). The proposed reaction proceeds as shown



in Eq. 1, where (I) represents the graphite fiber ( $\text{---G---}$ ) with adjacent hydroxyls at one portion of its surface; (II), the iodate complex; and finally, (III), the carbonyl-substituted fiber with reduction by-products.

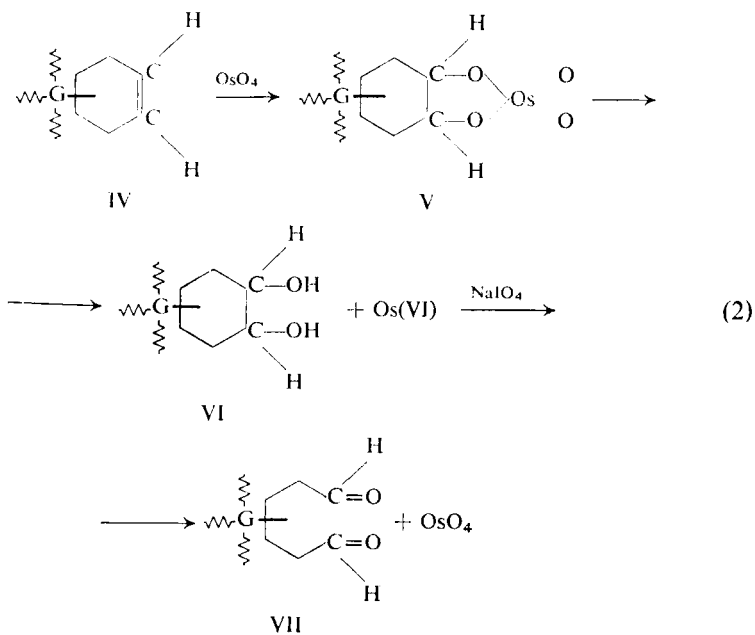
Schwartz<sup>9</sup> points out the possible danger of "overconsumption," a time-temperature effect which may be better characterized as simply, "overoxidation," where the carbonyl is further oxidized to carboxyl, and at the extreme, carbon dioxide.

## 2 OsO<sub>4</sub>/NaIO<sub>4</sub>

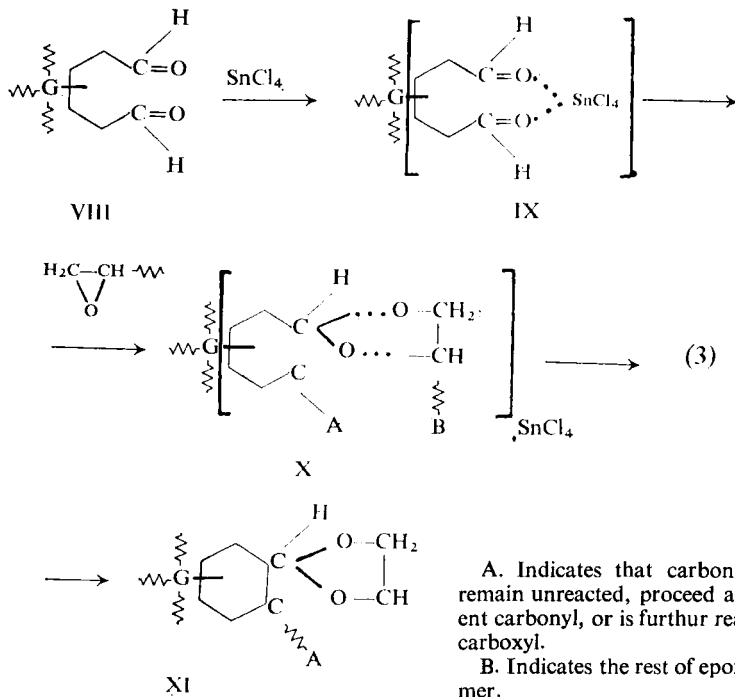
As mentioned earlier, unsaturation may exist on the fiber surface. Assuming this to be so, the writer postulates that hydroxyl efficiency may be increased (assuming hydroxyls already exist on the surface) by the reaction of OsO<sub>4</sub> with the carbon-to-carbon double bond, subsequently followed by a NaIO<sub>4</sub> conversion to carbonyls. A similar technique was followed by Oberender<sup>10</sup> in the oxidation of pyrene. The proposed mechanism shows the reaction of the OsO<sub>4</sub> with the graphite surface (IV) to form the osmate ester (V) complex which reverts to a surface containing 1,2-diols (VI) and reduction of the OsO<sub>4</sub> to the higher valence state metal. The presence of NaIO<sub>4</sub> (Malaprade Reaction) serves to oxidize the hydroxyls to carbonyls VII, and as a most important secondary effect, it oxidizes the Os to OsO<sub>4</sub>, thus forming a regenerative cycle (Equation 2)

## 3 Carbonyl-epoxy reaction

The final postulate needed to satisfy base conditions for further discussion is the mechanism for coupling the carbonylated graphite surface to the oxirane ring of the epoxy molecule. It is therefore stipulated that such a mechanism



happens through the formation of a stannic chloride (SnCl<sub>4</sub>) intermediate which proceeds (see Equation 3) by



reacting  $\text{SnCl}_4$  (in 2-butanone) with (VIII) to form a complex. Bogert<sup>10</sup> reported the formation of a solid complex in the reaction between aldehydes when using  $\text{SnCl}_4$  that dissolves as an ethylene oxide is added. Figure 15 (typical of all treatments after  $\text{SnCl}_4$  addition) also indicates formation of a

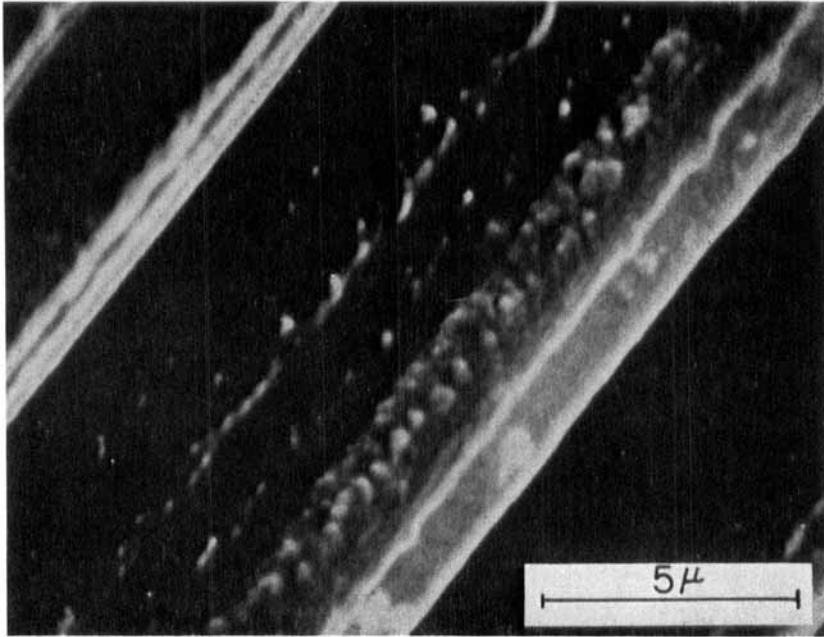


FIGURE 15 As received  $\text{H}_2\text{O}$  sized fiber after  $\text{SnCl}_4$ /2-butanone impregnation.

solid precipitate. Care must be used to interpret such an observation, since the possibility exists of forming colloidal stannic acid in the presence of atmospheric moisture. The latter is assumed not to occur. Addition of the polymer results in the intermediate (X), and finally a cyclized coupling shown as (XI).

#### 4 $\text{SnCl}_4$ /ERL 2256 reaction

Data were not readily available for the Lewis acid reaction with the ERL 2256 system, thus before proceeding with fiber treatments, appropriate amounts of catalyst, resin, and hardener needed to be determined to obtain optimum composite properties. Based on the results of composite tensile strand tests, a

solution composed of 0.2 ml  $\text{SnCl}_4$  in 50 ml 2-butanone was selected as the optimum intermediate treatment, which after air drying was coated with an epoxy matrix solution composed of 5 grams ERL 2256 + 1.4 grams ZYL 0820 hardener + 10 grams of 2-butanone.

## 5 Treatment procedure

A four-neck, 800-ml reaction vessel Figure 16; 4th stoppered neck not shown) was used to bulk treat the yarn. The Pyrex cylinder (4.5 inches long, 3.1 inches

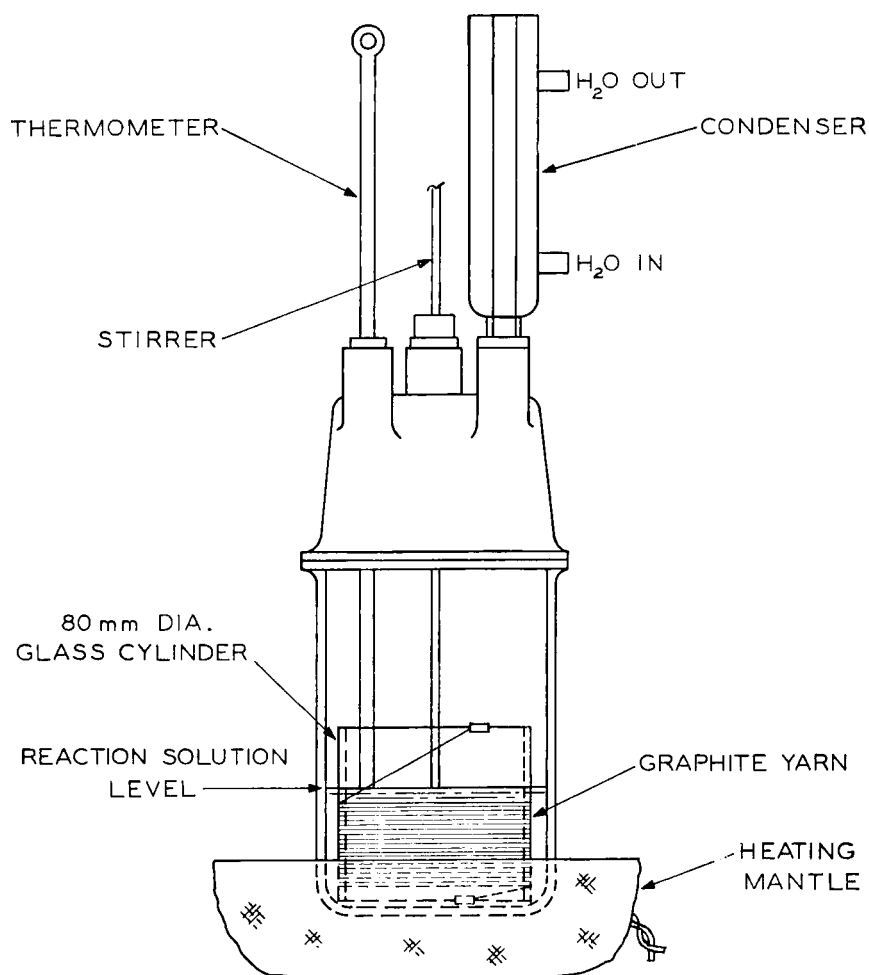


FIGURE 16 Reaction vessel with graphite yarn wrapped about glass cylinder.



OD) shown on the inside of the vessel was used to maintain yarn integrity during treatment and transfer from cylinder to volumetric and strand tests. The clamps used to hold the yarn (12½ to 15 feet) in place consisted of two short lengths (¼ inch) of polyethylene tubing which were slit lengthwise and pressed over the opposite ends of the cylinder, thereby compressing the end of the yarn between the slit tubing and glass surface. Solution temperatures were controlled by means of a rheostat connected to a heating mantle.

The reaction solutions consisted of

a)  $\text{NaIO}_4$  The reaction media for the  $\text{NaIO}_4$  treatments consisted of: 20 g  $\text{NaIO}_4$  (powdered with mortar and pestle) in 240 ml distilled  $\text{H}_2\text{O}$ .

Note: Modification of the above solution (see Table VI) were used for treating yarn to determine composite shear strength.

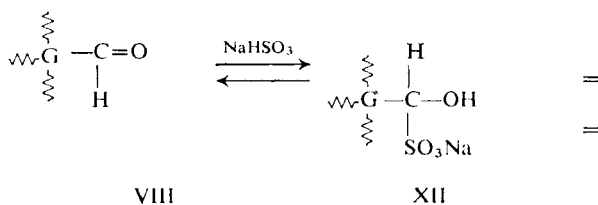
b)  $\text{OsO}_4/\text{NaIO}_4$  The reaction media for the  $\text{OsO}_4$  treatments consisted of: 20 g  $\text{NaIO}_4$  (powdered with mortar and pestle) 180 ml dioxane/60 ml  $\text{H}_2\text{O}$  where the amount of  $\text{OsO}_4$  varied from 0.1390 to 0.1549.

After each treatment (a or b), the yarns were washed with 500 ml of distilled  $\text{H}_2\text{O}$  and placed in a vacuum oven for a minimum drying time of one hour at 212°F. After drying, the yarns were analyzed for carbonyl as described in the following section.

## 6 Iodimetry

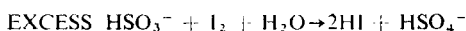
An iodimetric method of analysis was used to quantitatively determine the amount of carbonyl present on the graphitic fiber surface. Although other methods, as well as modifications of the experimenter's choice are available, this method was chosen because of its simplicity and material availability. Reference texts by Cheronis<sup>11</sup> and Schenk<sup>12</sup> were most useful in guiding the investigation.

Essentially, the graphite fibers were subjected to an aqueous solution of sodium bisulfite where the treated fibers VIII reacted to form XII.



VIII

XII



The unreacted bisulfite ion was then titrated with iodine solution (tri-iodide ion). It is apparent that to calculate the amount of carbonyl formed, "blank" solutions of sulfite ions (no fibers present) must be titrated to obtain by difference the volumetric amount of titrant which relates to the amount of carbonyl initially present. "Control" solutions of untreated fibers in aqueous bi-sulfite solutions were also titrated to obtain the increase in carbonyl formation (assuming that untreated fibers contain such functionality). Based on twelve sets of titrations, the average milliequivalent (meq) of carbonyl per gram of untreated Thornel 50 was  $-1.30$ . The negative sign may be attributed to the absence of carbonyl or the presence of trace amounts, which gives rise to data scatter as a result of inefficient operator technique and/or the overall sensitivity of the system. All reported data is in reference to the blank solutions.

## 7 Discussion

a.  $\text{NaIO}_4$  Treatment The aqueous  $\text{NaIO}_4$  treatment was very convenient to conduct, because it merely involved the addition of 20 grams of finely powdered  $\text{NaIO}_4$  to distilled  $\text{H}_2\text{O}$  or an aqueous dioxanes solvent, followed by the graphite fibers.

Figure 17 shows the result of subjecting the fibers to  $\text{NaIO}_4$  in a dioxane (180 ml)/ $\text{H}_2\text{O}$  (60 ml) solution at a temperature of  $82^\circ\text{C}$ . The resolution appears to be approaching the maximum (200 Å) with this photo (assuming 20,000 X is the true magnification) as calculated widths of the striations parallel to the fiber length are approximately 250 Å. More will be mentioned later in the discussion about these phenomena.

Average bundle tensile strength of composites fabricated with yarn treated by the  $\text{NaIO}_4$  method indicated that there was a maximum decrease from the control amounting to some 8.5%. Other treatments<sup>1,3</sup>, including gaseous oxidation and electrolytic oxidation, typically show decreases in tensile strength in excess of 19%.

Figure 18 graphically shows the results of the carbonyl analysis. Each point is an average of two titrations. The carbonyl data seem to be taking the direction of higher carbonyl content as time and temperature are increased. The dashed line is drawn to indicate a trend and by no means should be considered as "projected" data. Table V provides actual carbonyl meq per gram of Thornel 50, as well as time and temperature of treatment.

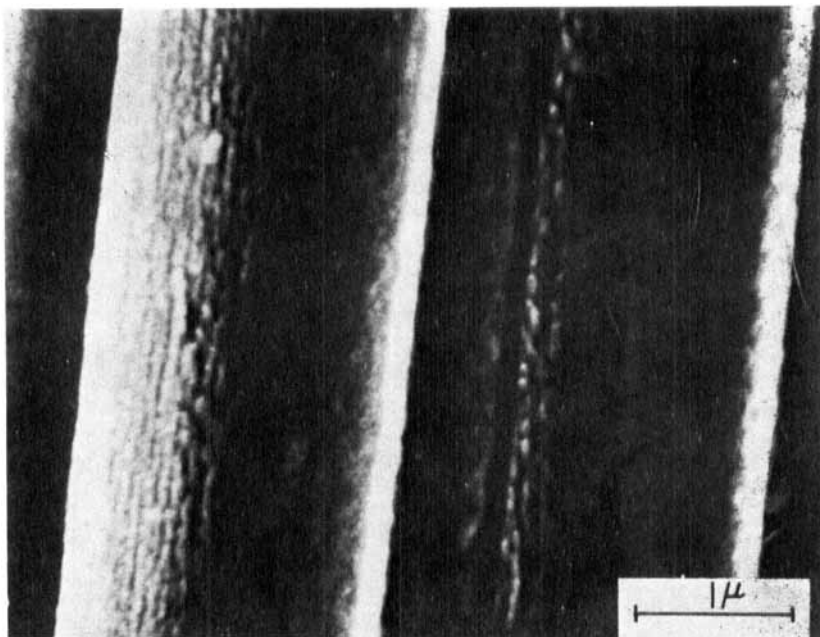


FIGURE 17  $\text{NaIO}_4/\text{H}_2\text{O}$  treatment; 8 hours at  $25^\circ\text{C}$ .

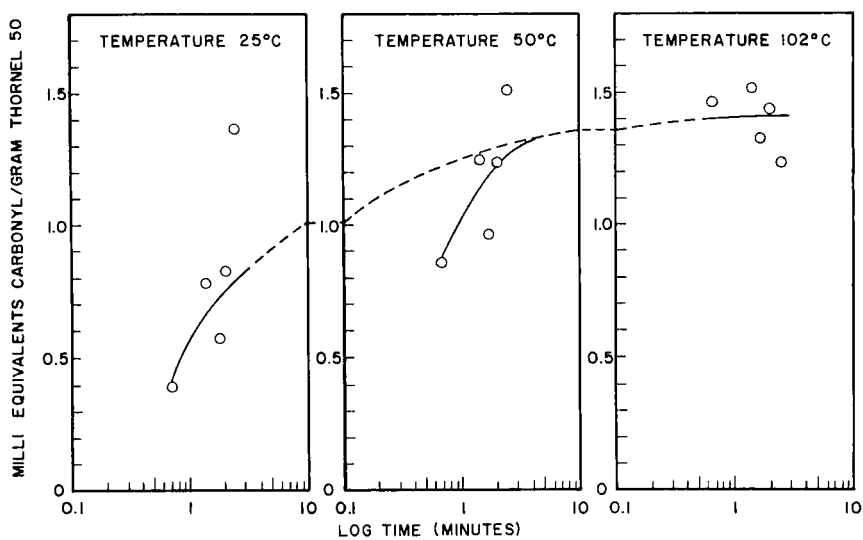


FIGURE 18 Milli equivalents carbonyl/gram thornel 50 Vs Log of reaction time at  $25^\circ\text{C}$ ,  $50^\circ\text{C}$ , and  $102^\circ\text{C}$ .

TABLE V  
Milliequivalents of carbonyl per gram of Thornel 50 graphite  
fibers via  $\text{NaIO}_4$  solution treatment

	Treatment number	Treatment time (minutes)	Milli- equivalents per gram
at 25°C	30-1	5	0.44
	30-2	5	0.34
	33-1	30	0.63
	33-2	30	0.88
	31-1	60	0.41
	31-2	60	0.71
	32-1	120	0.74
	32-2	120	0.89
	29-1	480	1.59
	29-2	480	1.12
at 50°C	34-1	5	0.96
	34-2	5	0.77
	28-1	30	1.42
	28-2	30	1.07
	27-1	60	0.38
	27-2	60	1.53
	26-1	120	1.35
	26-2	120	1.15
	25-1	480	1.52
	25-2	480	1.44
at 102°C	24-1	5	2.03
	24-2	5	0.85
	23-1	30	1.59
	23-2	30	1.43
	22-1	60	1.59
	22-2	60	1.03
	21-1	120	1.35
	21-2	120	1.46
	20-1	480	1.65
	20-2	480	0.77

Other than the composite tensile strand data, only a limited amount of composite fabrication and testing with treated yarns has been accomplished. Table VI shows that composite interlaminar shear strength is improved via a  $\text{NaIO}_4$  treatment. In the examples shown, instead of an totally aqueous solution, it was modified by addition of dioxane.

b.  $\text{OsO}_4/\text{NaIO}_4$  Treatment The average bundle strength decrease of all yarns treated by the  $\text{OsO}_4/\text{NaIO}_4$  method was minimal at 6.2%. Even at the

lowest average of  $223 \times 10^3$  psi, for a particular treatment, only a 13% loss in strength is in effect.

The  $\text{OsO}_4/\text{NaIO}_4$  reaction was more difficult to regulate than the reaction because of the danger involved in the handling of the high vapor pressure, toxic  $\text{OsO}_4$ . Catalytic amounts of  $\text{OsO}_4$  were weighed on a microbalance in a well ventilated hood. The  $\text{OsO}_4$  sublimed readily and the weights of tetroxide shown in Table VII are indicative of the last weights recorded before deposition into the reaction vessel. Actual weights are probably a few tenths of a milligram to one milligram less than those recorded.

TABLE VI  
Composite short beam shear strengths span to depth ratio 4/1  
 $\text{NaIO}_4$  Treatment

Composite	Treatment solution	Treatment time (min)	Treatment temp. ( $^{\circ}\text{C}$ )	Composite shear strength $10^3$ psi
A	34.0 g $\text{NaIO}_4$ 100 ml $\text{H}_2\text{O}$ 180 ml Dioxane	30	88	6.4
				6.4
				6.4
				Avg. 6.4
B	54.5 g $\text{NaIO}_4$ 225 ml $\text{H}_2\text{O}$ 100 ml Dioxane	160	88	5.5
				5.2
				5.0
				5.2
C	54.5 g $\text{NaIO}_4$ 225 ml $\text{H}_2\text{O}$ 100 ml Dioxane	160	88	5.5
				5.8
				5.5
				5.6

Since the process was a regenerative one, initial ingredients were used for a series of experiments as may be gathered from Table VII where different treatment numbers have the same weight of  $\text{OsO}_4$  tabulated. This, however, presented an additional problem because the concentration of solids in subsequent treatments (using the same starting formulation) was not exactly known, and since after each subjection of yarn to treatment, the yarn was washed over the open end of the reaction vessel. Thus, for treatment number 6, assuming approximately 25 ml of a dioxane/ $\text{H}_2\text{O}$  solution was used for each wash, the reaction formulation may be diluted by as much as 75 ml. Treatment numbers that are the same indicate that two samples from the same processed yarn were analyzed for carbonyl content.

TABLE VII  
Milliequivalents of carbonyl per gram of Thornel 50 graphite fibers  
via  $\text{OsO}_4/\text{NaIO}_4$  solution treatment

	Treatment number	Weight $\text{OsO}_4$ (grams)	Treatment time (min.)	Milli-equivalents per gram	
at 25°C	3	0.1547	1	— <sup>a</sup> 0.062	
	4	0.1547	5	0.10	
	5	0.1547	15	0.39	
	6	0.1547	30	1.05	
	7	0.1509	60	0.21	
	8	0.1509	120	0.08	
	9	0.1509	15	0.61	
	at 48°C	10-1	0.1390	5	0.08
		10-2	0.1390	5	0.00
at 71°C	11-1	0.1315	5	—0.13	
	11-3	0.1315	5	—0.19	
at 84°C	12-1	0.1549	5	0.19	
	12-2	0.1549	5	—0.79	
at 55°C	13	0.1549	120	—0.45	
at 88°C	14	0.1459	5	0.00	

<sup>a</sup> Indicates that volumetric amount of titrant was greater for treated sample than blank.

At 25°C, even with the dilution of the tetroxide, there is an increase in the meq of carbonyl up to a period of  $\frac{1}{2}$  hour. The reaction mixture was changed and a noticeable decrease in carbonyl content was observed for the 1-hour reaction time even though the  $\text{OsO}_4$  concentration differed little from the starting concentration of the previous series of treatment. As the temperature of the process was increased, carbonyl analysis proved negative.

There seems to be a time-temperature relationship with longer times and higher temperatures being detrimental to carbonyl formation. The deciding influence may be the dioxane in solution which could form compounds of the peroxide type which could in turn overoxidize the carbonyls to carboxyls, or carbon dioxide. Precautions as outlined by Fieser<sup>13</sup> were followed to reduce the possibility of forming unwanted peroxides, but at higher temperatures, the increase in thermal energy may be enough to activate the peroxide formation mechanism spontaneously. Thus, contrary to the  $\text{NaIO}_4$  treatment, in which increasing temperatures enhance carbonyl content, the  $\text{OsO}_4/\text{NaIO}_4$  treatment at elevated temperatures has the opposite effect. The combination of ingredients, including dioxane, rapidly oxidizes the graphite at higher temperatures, and results in a fine-grained surface.

Other than the tensile strand data alluded to, only preliminary composite properties (Table VIII) were obtained which showed a marginal improvement in composite shear strength over "control" composites.

TABLE VIII  
Composite short beam shear strengths span to depth ratio 4/1  
OsO<sub>4</sub>/NaIO<sub>4</sub> treatment

Composite	Treatment solution	Treatment time (min)	Treatment temp (°C)	Composite shear strength 10 <sup>3</sup> psi
D	0.2125 g OsO <sub>4</sub> 30.0 g NaIO <sub>4</sub> 170 ml H <sub>2</sub> O	30	70-72	4.9
				4.2
				4.8
				Avg. 4.6
E	0.2125 g OsO <sub>4</sub> 30.0 g NaIO <sub>4</sub> 170 ml H <sub>2</sub> O 150 ml Dioxane	3	65	5.1
				4.8
				4.7
				Avg. 4.9

c. *Surface Morphology* The idealistic schematics shown in Figure 19 are based on observations made via the scanning electron photomicrographs. Only a portion of the crenulated 5  $\mu$ -diameter fiber is shown. The schematic implies that prior to oxidative etch, the surface contain large ordered areas of the dimensions shown. These grains, separated by grain boundaries, were indistinguishable with SEM (Figure 3 and 4) because of the limited resolving power (200 Å) of the instrument. Because of the high energy<sup>14</sup> associated with grain boundaries, they are susceptible to oxidative attack and, as oxidation proceeds via the subject treatment(s), the boundaries are progressively etched away, thus causing the fiber surface to assume the somewhat nodular appearance shown in the actual photomicrograph (Figure 20; refer also to Figure 17) and portrayed in the schematic.

The cutout further indicates that the large grains are composed of crystallites of the type, but not necessarily of the dimensions, posed by Johnson and Tyson<sup>14</sup>. Here, crystallite boundaries and voids, also of high energy, are amenable to oxidative attack. The irregular topography of individual grains is attributed to oxidation of crystallite boundaries.

Johnson and Tyson<sup>14</sup> claim that the fibrillar theory has been overemphasized as the primary explanation for overall fiber morphology. In their study,

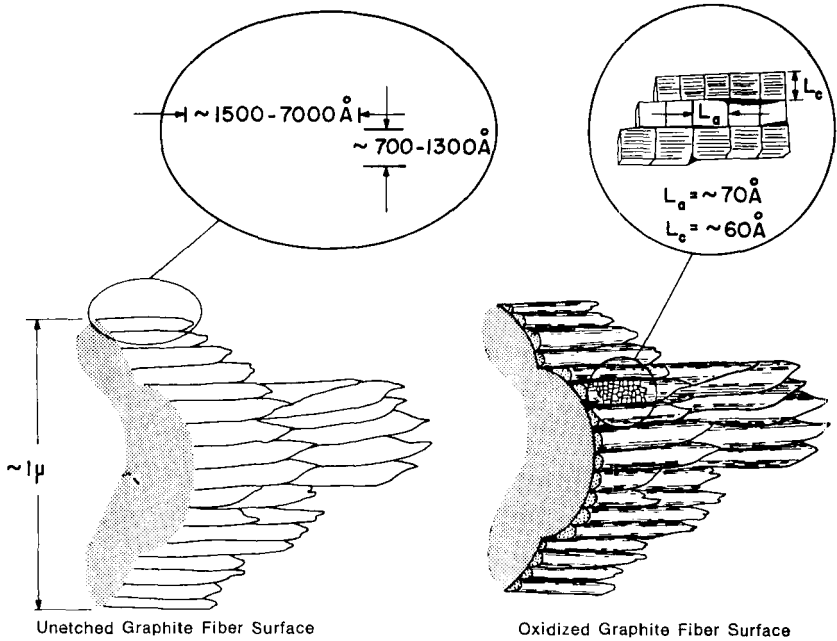


FIGURE 19 Portion of graphite fiber surface before and after oxidative etch.

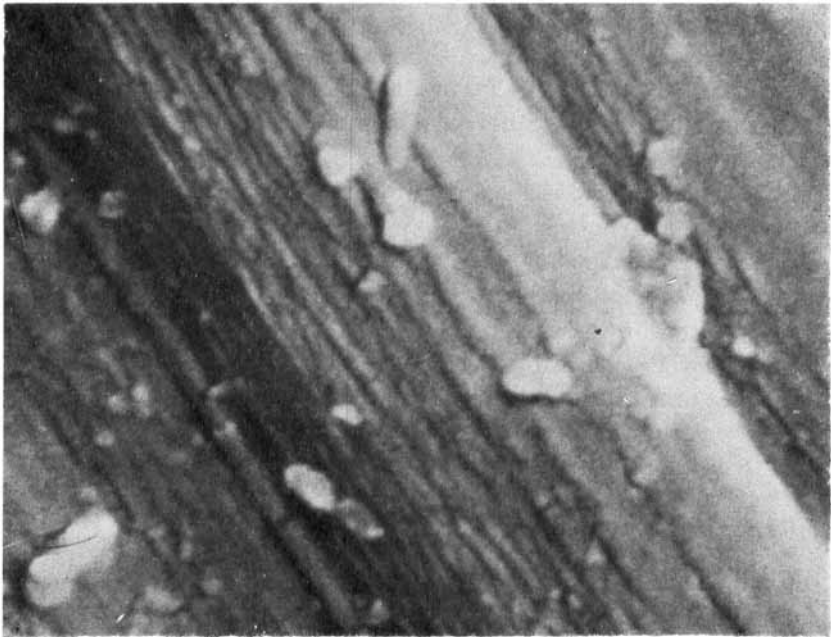


FIGURE 20 Treatment 22;  $\text{NaIO}_4/\text{H}_2\text{O}$ , 1 hour at  $102^\circ\text{C}$  ( $20,000\times$ ).



they advocate a fiber composed of crystallites with tilt and subgrain boundaries. In a later study, Johnson<sup>15</sup> reported that individual layers of crystallites "may well be much longer" than 100 Å

Diefendorf<sup>16</sup> recently has shown through replication transmission microscopy that graphite fibers oxidatively treated by other methods produce similar effects, as described by this writer. In his study, he refers to the grains as ridges on the fiber surface.

The writer hypothesizes that the surface of graphite fibers (Thornel 50) is not rigorously fibrillar, nor crystallite but is, instead, a compromise of crystallites (with tilt and subgrain boundaries) that may be ordered over large distances within grains. The degree (length) of order as determined by direct resolution of lattice planes<sup>17</sup> may give rise to descriptions which erroneously imply a crystallite order ad infinitum.

## V CONCLUSIONS

### 1 Heat treatment-polymeric coating

Initial data indicated that a simple heat treatment (propane torch) followed by solution coating with a thermoplastic resin would improve epoxy/graphite composite shear strength without significant adverse effects on fiber mechanical properties. Such a treatment would be most attractive from economics and ease of production criteria. On compilation of pertinent processing parameters, polymeric coating solutions, and composite mechanical and physical property data, the following statements may be made:

a) Heat treatment alone does not appear to improve composite shear strength.

b) Polymeric coating in the absence of heat treatment does not improve composite shear strength.

c) The experimental data indicates that a combination of a propane flame heat treatment and polymeric coating prior to epoxy matrix impregnation will improve composite shear strength of PVA or H<sub>2</sub>O-sized Thornel graphite composites by about a factor of two or more.

d) SEM evaluations of fractured composites vividly illustrated the presence on a great deal of elongated, material coming from within the fibers (both  $50 \times 10^6$  modulus yarns) used in this study.

### 2 Chemical processes

The results of this phase of study indicate that:

a) An aqueous sodium iodate (NaIO<sub>4</sub>) treatment imparts carbonyl functionality to high modulus graphite fibers.

- b) The amount of carbonyl formed is a function of time and temperature.
- c) A coarse-grained fiber surface results when subjected to  $\text{NaIO}_4$  for moderate lengths of time or high temperature.
- d) The aqueous  $\text{OsO}_4$ - $\text{NaIO}_4$  dioxane treatment also forms carbonyls, but only at room temperature solution ( $25^\circ\text{C}$ ).
- e) The  $\text{OsO}_4$  treatment at elevated temperature induces a fine-grained appearance to the graphite fiber surface which is probably accelerated by dioxane.
- f) Both treatments enhance epoxy-resin/graphite-fiber adhesion as observed from SEM photomicrographs of fractured surfaces of composite tensile specimens.
- g) Degradation of fiber properties, as a result of both treatments, is minor.
- h) Appearance of the grainy fiber surface may be due to preferential attack of oxidizers at grain boundaries which encompass large ordered areas or graphite crystallites.
- i) The highly ordered areas may be oriented more or less parallel to the fiber axis (tilt) and/or twisted with respect to immediate neighboring grains.
- j) The grain boundaries are sites of high energy and are susceptible to attack by a variety of oxidants.
- k) Crystallites of the type described by Johnson and Tyson<sup>14</sup> are present within these large grains and are also subject to oxidative attack at crystallite subgrain boundaries, thus causing the irregular surface of grains viewed by SEM.
- l) Pores<sup>15 18</sup> which separate crystalline regions within the fiber also contribute to the etch markings which are a result of oxidation.
- m) Both wet chemical processes improve composite interlaminar shear strength.
- n) The highly toxic osmium tetroxide poses production problems in scaling the batch process to a continuous in-line operation.

## References

1. R. Didchenko, *Carbon and Graphite Surface Properties Relevant to Fiber Reinforced Composites*, AFML-TR-68-45, February, 1968.
2. J. Bickerman, *The Science of Adhesive Joints*, 2nd Edition (Academic Press, N.Y., 1968).
3. Private communication with D. Fox; General Electric, 13 April, 1970.
4. E. H. Andrews, *Fracture in Polymers* (American Elsevier Publishing Co., New York, 1968).
5. R. Kuhbander, *Determining Fiber Content of Graphite Yarn-Epoxy Resin Composites*, AFML-TR-67-243, August, 1967.
6. J. Johnson, *Applied Polymer Symposia* **9**, (1969).

7. L. Malaprade, *Compt. Rend. Acad. Sci.* **186**, 382 (1928).
8. K. Wiberg, *Oxidation in Organic Chemistry*, Vol. 5-A (Academic Press, N.Y. 1965).
9. J. Schwartz, and M. MacDougall, *J. Chem. Soc.* 3065 (1956).
10. F. Oberender, and J. Dixon, *J. Org. Chem.* **24**, 1226 (1959).
11. N. Cheronis, and T. Ma, *Organic Functional Group Analysis by Micro and Semi-micro Methods* (Interscience Publishers, 1964).
12. G. Schenk, *Organic Functional Group Analysis Theory and Development* (Pergamon Press, New York, 1968).
13. L. Fieser, *Experiments in Organic Chemistry*, 2nd Edition (D. C. Heath and Co, Boston, 1950), p. 368.
14. D. Johnson, and C. Tyron, *Brit. J. Appl. Phys., Ser. 2*, **2**, 787 (1969).
15. D. Johnson, *Nature* **226**, 750 (1970).
16. R. Diefendorf, B. Butler, C. LeMastre, *Structure of High Modulus Graphite Fibre* presented at Symposium on Surface Chemistry of Composite Materials 163rd, American Chemical Society Meeting, Boston Mass., April (1972).
17. J. Hugo, V. Phillips, B. Roberts, *Nature* **226**, 144 (1970).
18. R. Bacon, and M. Tang, *Carbon* **2**, 225 (1964).